Kumar et al., Supplementary Information

Intrinsic suppression of type I interferon production underlies the therapeutic efficacy of IL-15-producing natural killer cells in B-cell acute lymphoblastic leukemia

Supplementary Figures 1-15

Supplementary Tables 1-5

Figure S1: *Concomitant high expression of IFN-I production and IFN-I signaling/response transcripts predicts favorable clinical prognosis in patients with B-ALL.*

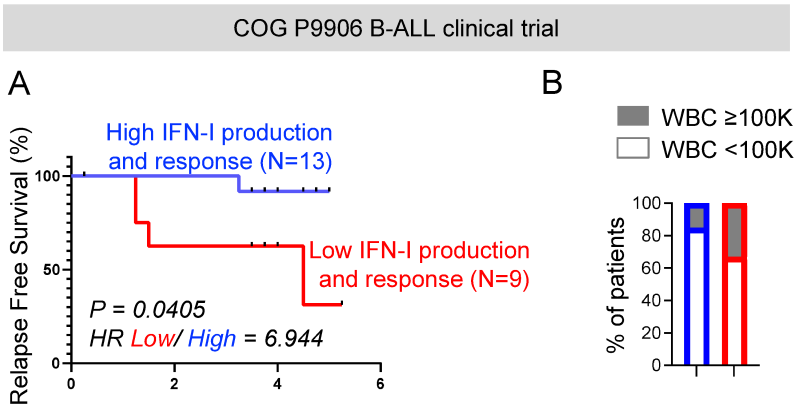

Figure S1: Concomitant high expression of IFN-I production and IFN-I signaling/response transcripts predicts favorable clinical prognosis in patients with B-ALL. (A) Comparison of survival probabilities of COG P9906 B-ALL patients separated into 2 groups based on the median transcript expressions of IFN-I production (CD123 and IRF7) and IFN-I signaling/ response (IFNAR1, IFNAR2, STAT1, OAS1, MX1) genes as 'High IFN-I production and response' (n=13) and 'Low IFN-I production and response' (n=9). **(B)** Stacked bar charts comparing the proportions of COG P9906 B-ALL patients with WBC count ≥ 100 000 or WBC count < 100 000 within the 'High IFN-I production and response' and 'Low IFN-I production and response' cohorts. Survival was calculated by Kaplan-Meier method. p-value was calculated by the log-rank test. HR = Hazard ratio.

Figure S2: *Gating strategy for flow cytometry analysis of human PBMCs*

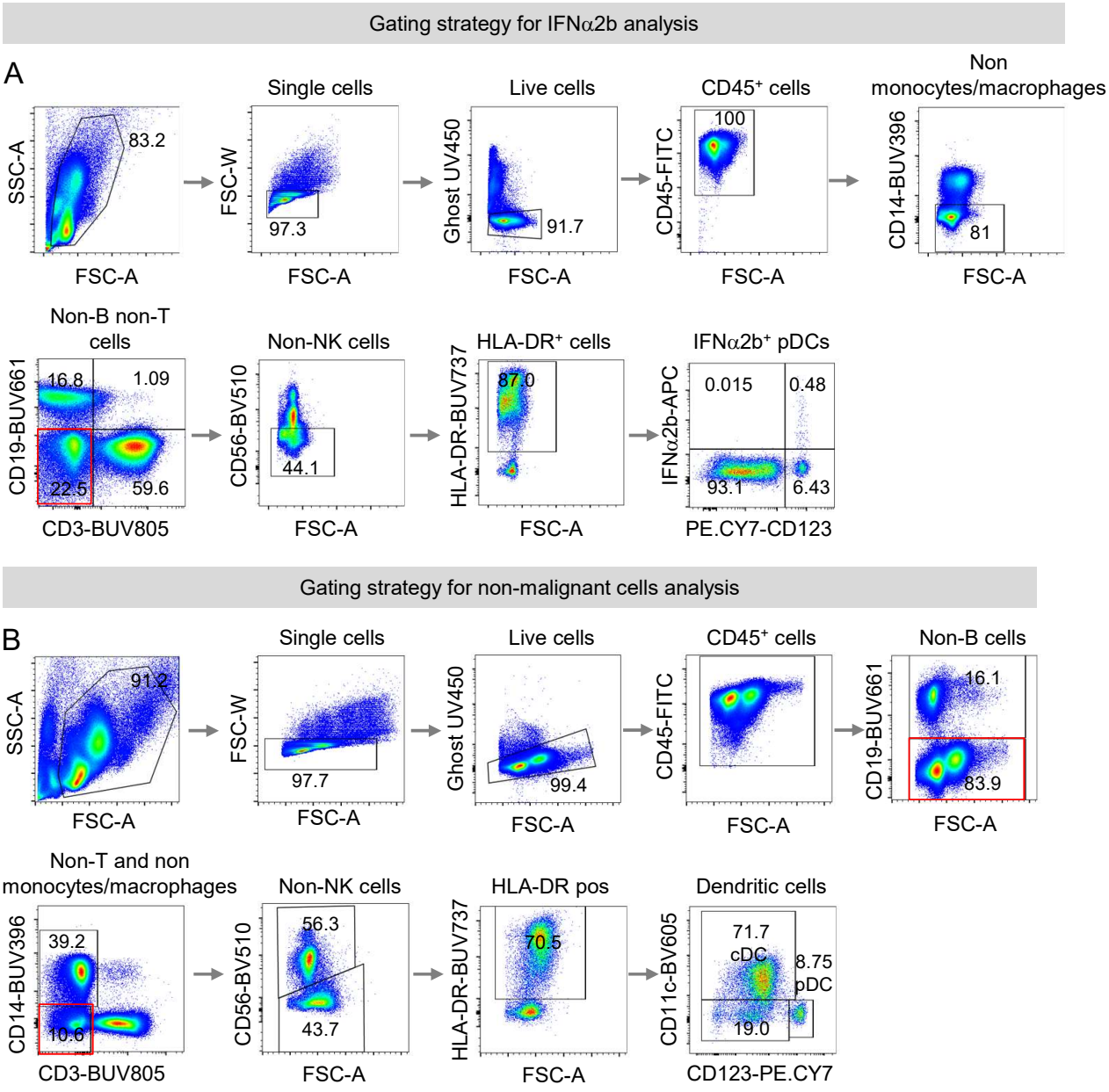

Figure S2: Gating strategy for flow cytometry analysis of human PBMCs. (A) For analysis of IFNα2b-expressing immune cells, lymphocytes were gated based on forward and side scatter of the cells followed by gating of singlets and selection of live cells as Ghost-UV450$^-$ and leucocytes as CD45$^+$ cell fraction. Monocytes were then gated out (CD14$^-$ gate), followed by selection of non-B and non-T cells (CD19$^-$ CD3$^-$) and non-NK cells (CD56$^-$). HLA-DR$^+$ cells within the 'non-B, non-T, non-monocyte, and non-NK' fraction were analyzed for IFNα2b expression. **(B)** For calculating frequencies of DC subsets within the non-leukemic immune cell fraction (CD19$^-$), live leucocytes were selected as in (A) followed by selection of CD19$^-$ immune cells. Then HLA-DR$^+$ cells were selected within non-monocytes, non-T, and non-NK cells and frequencies of cDCs, pDCs, and non-cDC/non-pDC were analyzed.

Figure S3: *Reduction in frequencies of IFN-Is producers (pDC) in the BM of B-ALL patients*

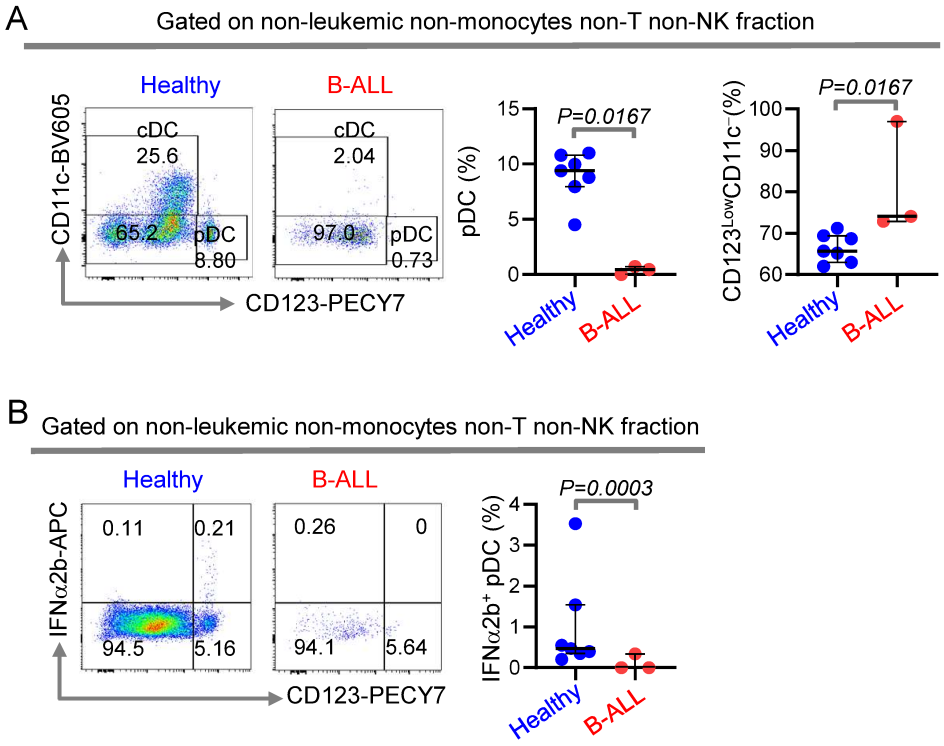

Figure S3: **Reduction in frequencies of IFN-Is producers (pDC) in the BM of B-ALL patients (A)** Comparison of bone marrow pDC frequencies within the non-B, non-monocytes, non-T, non-NK, and HLA-DR$^+$ immune cell fractions between B-ALL patients (n=3) and healthy donors (n=7) by flow cytometry. **(B)** Comparison of IFNα2b$^+$ cells within the HLA-DR$^+$ non-B, non-T, non-monocytes, and non-NK immune cell fraction of BMMC after stimulation with class C CpG ODN between B-ALL patients (n=3) and healthy donors (n=7) by flow cytometry. All pairwise comparisons between any two groups were conducted using the Mann-Whitney U test. Exact p-values are provided whenever significant (<0.05) or trending to significance (0.05<p<0.1).

Figure S4: *Gating strategy for CyTOF analysis of T-cell subsets in PBMC.*

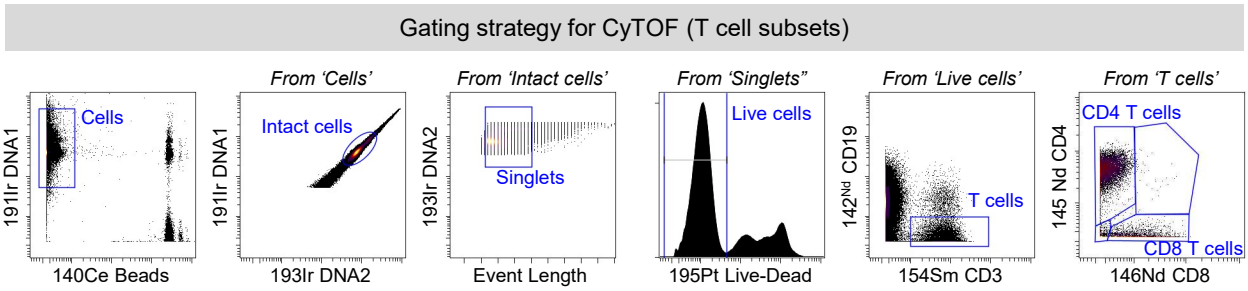

Figure S4: Gating strategy for CyTOF analysis of T-cell subsets in PBMC. From live intact singlet populations, $CD3^{+}CD19^{-}$ cells were selected to get the non-leukemic fraction and analyzed for the frequencies of $CD4^{+}$ and $CD8^{+}$ cells.

Figure S5: *HLA-DR expression is reduced on leukemic B cells compared to their healthy counterparts.*

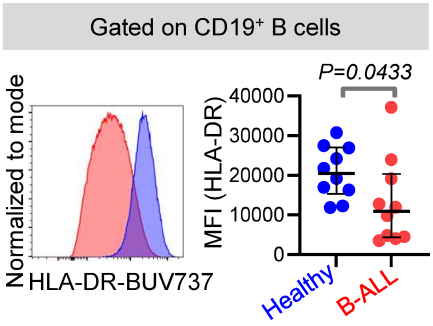

Figure S5: HLA-DR expression is reduced on leukemic B cells compared to their healthy counterparts. Representative histogram overlay and dot plots depicting median fluorescence intensity of HLA-DR expression on B cells of B-ALL patients (n=10) and healthy donors (n=10).

Figure S6: *Magnetic sorting of leukemic (B-cell) and non-leukemic (non-B) cell fractions from mouse splenic WBCs*

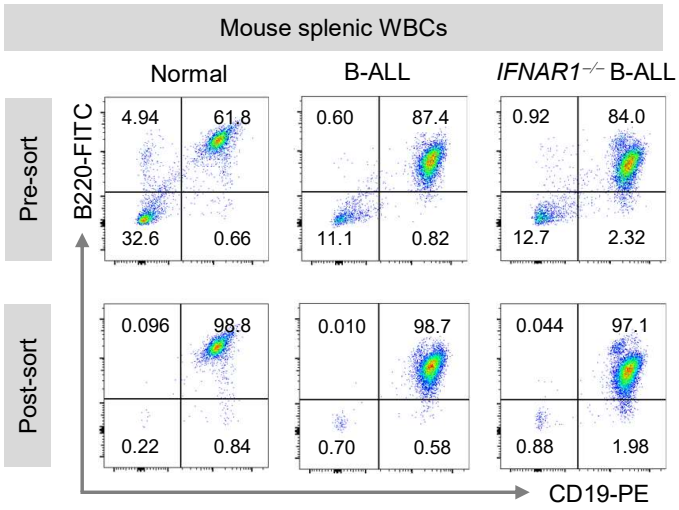

Figure S6: Magnetic sorting of leukemic (B-cell) and non-leukemic (non-B) cell fractions from mouse splenic WBCs. Representative flow cytometry plots showing the pre-sort and post-sort purity of murine splenic B-cell fractions from healthy, *Eμ-MYC* B-ALL-bearing, and *IFNAR1*$^{-/-}$ *Eμ-MYC* B-ALL-bearing mice after magnetic-activated cell sorting.

Figure S7: *Production of IFNβ is suppressed in bone marrow during primary B-cell leukemogenesis*

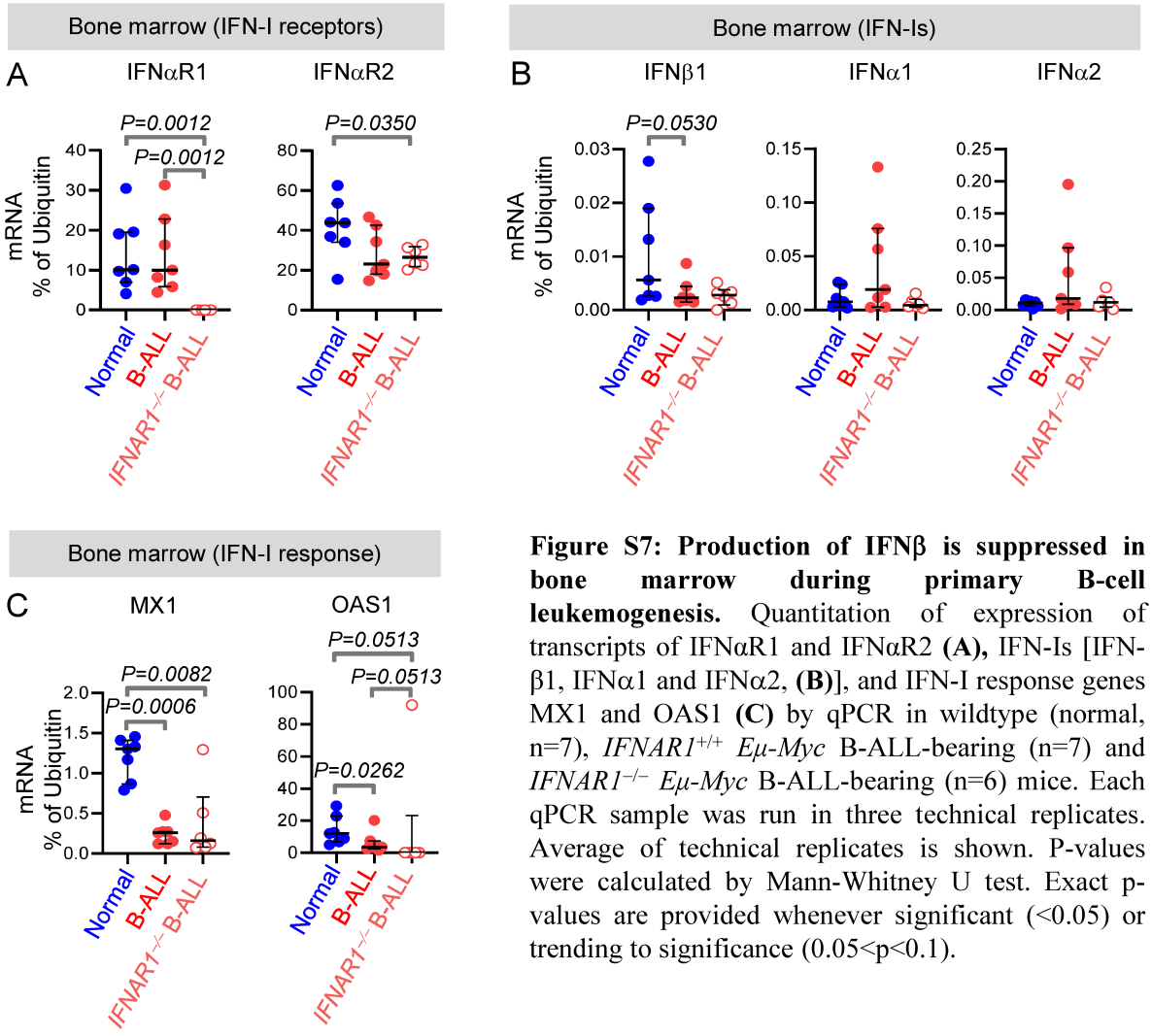

Figure S7: Production of IFNβ is suppressed in bone marrow during primary B-cell leukemogenesis. Quantitation of expression of transcripts of IFNαR1 and IFNαR2 **(A),** IFN-Is [IFN-β1, IFNα1 and IFNα2, **(B)**], and IFN-I response genes MX1 and OAS1 **(C)** by qPCR in wildtype (normal, n=7), *IFNAR1*$^{+/+}$ *Eμ-Myc* B-ALL-bearing (n=7) and *IFNAR1*$^{-/-}$ *Eμ-Myc* B-ALL-bearing (n=6) mice. Each qPCR sample was run in three technical replicates. Average of technical replicates is shown. P-values were calculated by Mann-Whitney U test. Exact p-values are provided whenever significant (<0.05) or trending to significance (0.05<p<0.1).

Figure S8: *IFN-I response is suppressed in leukemic and non-leukemic fractions during primary B-ALL development*

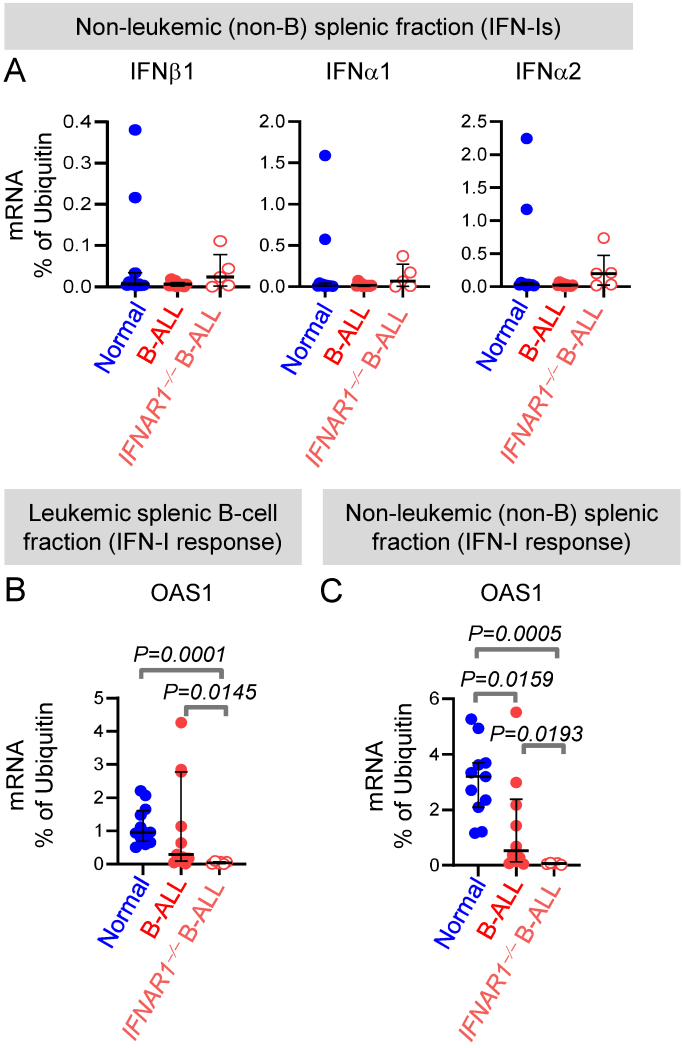

Figure S8: IFN-I response is suppressed in leukemic and non-leukemic fractions during primary B-ALL development. (A) qPCR quantitation of transcripts of IFNβ1, IFNα1, and IFNα2 in splenic non-B cell fraction of wildtype (normal, n=7), *IFNAR1*$^{+/+}$ *Eμ-Myc* B-ALL-bearing (spleen, n=10) and *IFNAR1*$^{-/-}$ *Eμ-Myc* B-ALL-bearing (n=5) mice. **(B-C)** qPCR quantitation of transcripts of OAS1 in leukemic (B) and non-leukemic (C) fractions of the spleen of wildtype (normal, n=12), *IFNAR1*$^{+/+}$ *Eμ-Myc* B-ALL-bearing (n=11) and *IFNAR1*$^{-/-}$ *Eμ-Myc* B-ALL-bearing (n=6) mice. P-values were calculated using Mann-Whitney U test. Exact p-values are provided whenever significant (<0.05) or trending to significance (0.05<p<0.1).

Figure S9: *Gating strategy for flow cytometry analysis of mouse immune cells.*

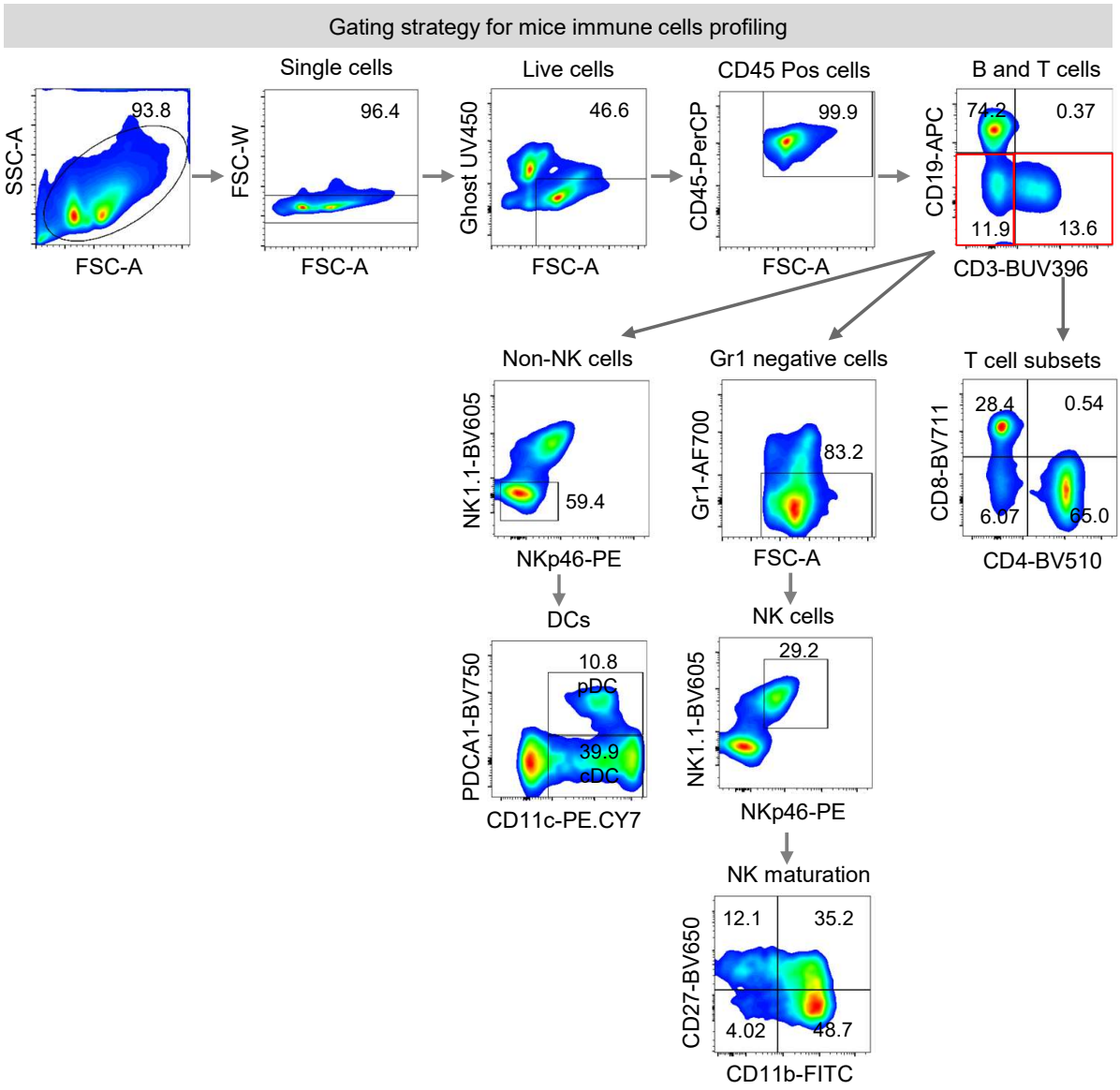

Figure S9: Gating strategy for flow cytometry analysis of mouse immune cells. From the lymphocytes cluster, singlets were gated followed by selection of live cells as Ghost-UV450^{-} and leucocytes as CD45^{+} cell fraction. T-cell subsets were analyzed from CD19^{-}CD3^{+} cells. After the selection of non-B (non-leukemic) and non-T cells, NK cells were analyzed after gating on Gr1^{-} fraction. cDCs and pDCs were analyzed from the non-NK fraction.

Figure S10: *Ablation of IFNAR1 does not exacerbate suppression of splenic T and DC subsets.*

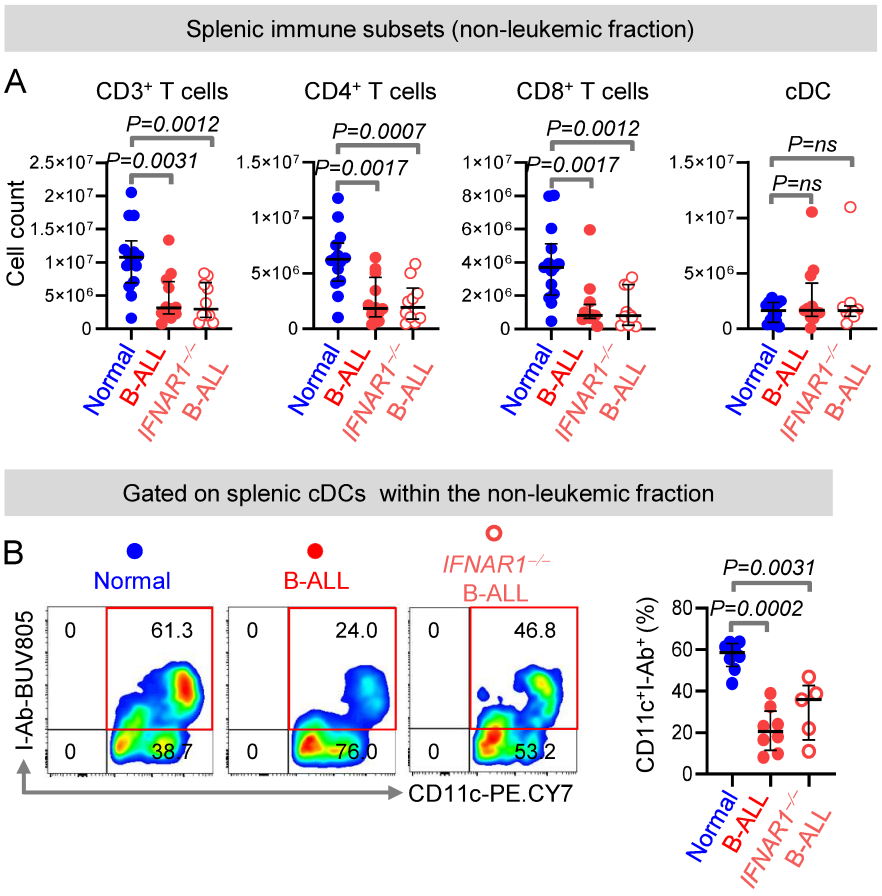

Figure S10: Ablation of IFNAR1 does not exacerbate suppression of splenic T and DC subsets. (A) Comparison of pan T cells, T-cell subsets, and cDC counts in the non-leukemic fraction of the spleen of normal (n=14), *IFNAR1*$^{+/+}$ *Eμ-Myc* B-ALL-bearing (n=12) and *IFNAR1*$^{-/-}$ *Eμ-Myc* B-ALL-bearing (n=10;) mice. **(B)** Flow cytometry measurement of frequencies of I-Ab^{+} cells within pan DC (CD11c^{+}) cells in the non-B, non-T, and non-NK cell fraction of the spleen of normal (n=8), *IFNAR1*$^{+/+}$ *Eμ-Myc* B-ALL-bearing (n=8), and *IFNAR1*$^{-/-}$ *Eμ-Myc* B-ALL-bearing (n=5) mice. P-values were calculated using Mann-Whitney U test. Exact p-values are provided whenever significant (<0.05) or trending to significance (0.05<p<0.1). ns = not significant.

Figure S11: *Bone marrow T-cell subsets are reduced only upon by IFNAR1 ablation during primary B-ALL development*

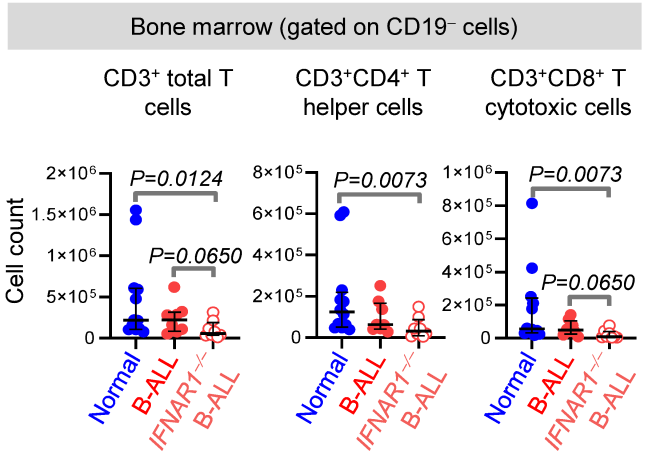

Figure S11: Bone marrow T-cell subsets are reduced only upon IFNAR1 ablation during primary B-ALL development. Comparison of pan T cells and T-cell subsets in the non-leukemic fraction of the bone marrow of normal (n=12), *IFNAR1*$^{+/+}$ *Eμ-Myc* B-ALL-bearing (n=8), and *IFNAR1*$^{-/-}$ *Eμ-Myc* B-ALL-bearing (n=8) mice. Comparisons were conducted using Mann-Whitney U test. Exact p-values are provided whenever significant (<0.05) or trending to significance (0.05<p<0.1).

Figure S12: *Purity of sorted mouse splenic NK cells used for NK adoptive transfer into ALL-bearing mice*

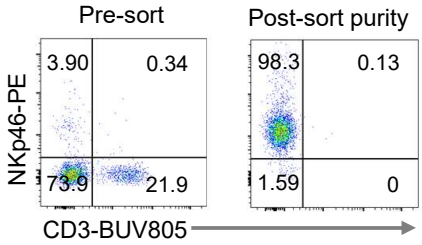

Figure S12: Purity of sorted mouse splenic NK cells used for NK adoptive transfer into ALL-bearing mice. Representative flow cytometry plots showing the pre-sort and post-sort purity of murine splenic NK cells isolated from normal syngeneic mice using magnetic-activated cell sorting.

Figure S13: *IFN-Is drive NK surveillance and reduce progression of B-ALL*

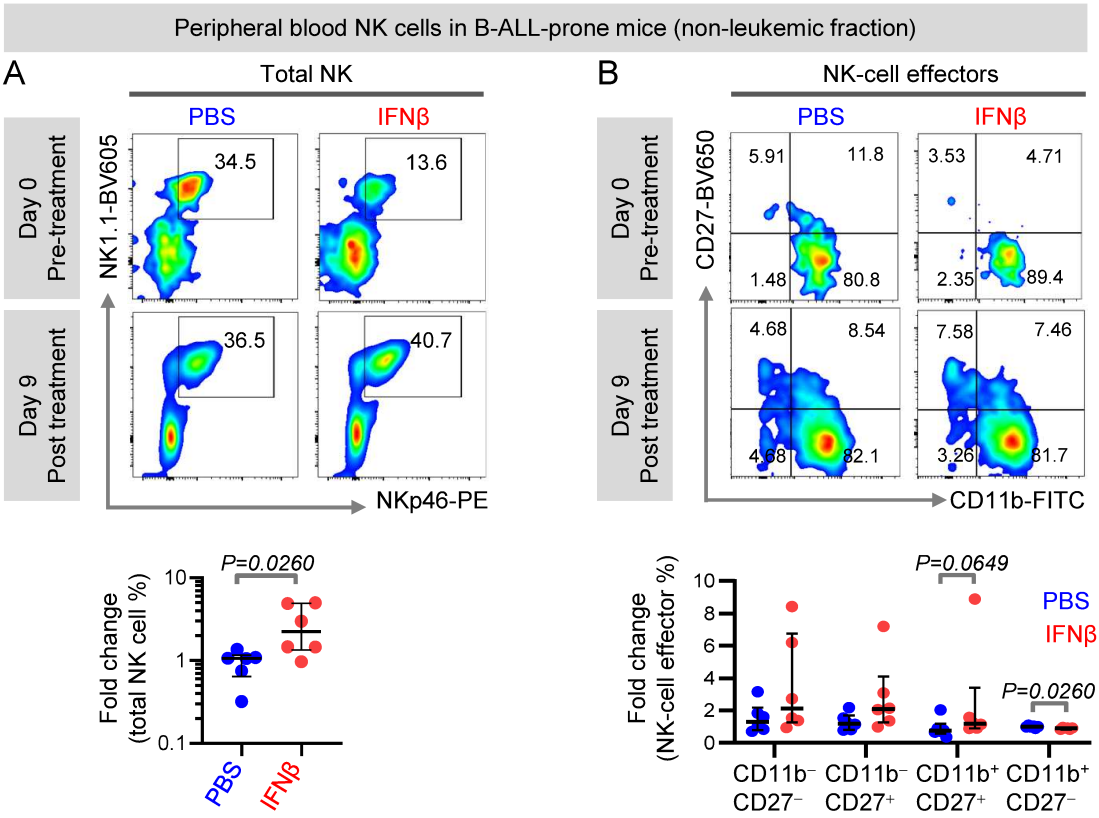

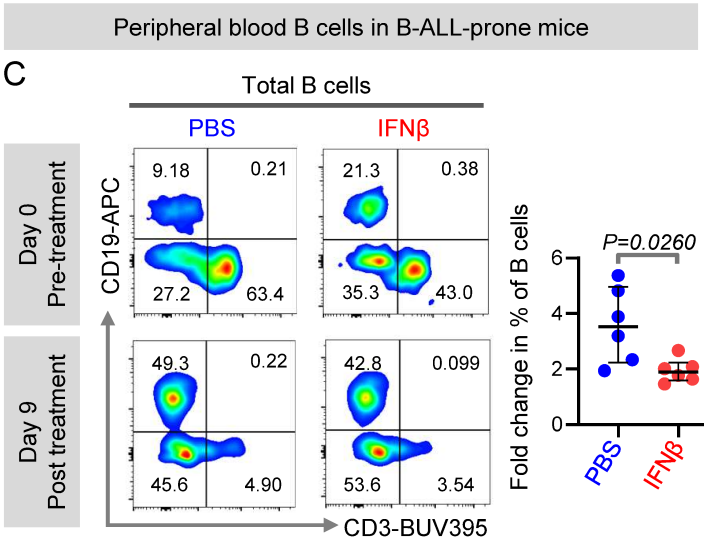

Figure S13: IFN-Is drive NK surveillance and reduce progression of B-ALL. Comparison of fold change in the frequencies of circulating total NK cells (A), NK effector subsets (B), and B-cells (C) in 7-20-week-old B-ALL-prone *Eμ-MYC* mice before (day 0) and after treatment (day 9) with PBS (control) or IFNβ. All fold changes are represented as ratio of day 9 IFN-β treatment : day 0 no treatment. P-values were calculated using Mann-Whitney U test. Exact p-values are provided whenever significant (<0.05) or trending to significance (0.05<p<0.1).

Figure S14: *CRISPRa-engineered IL-15 NK cells are not toxic to healthy donor PBMC*

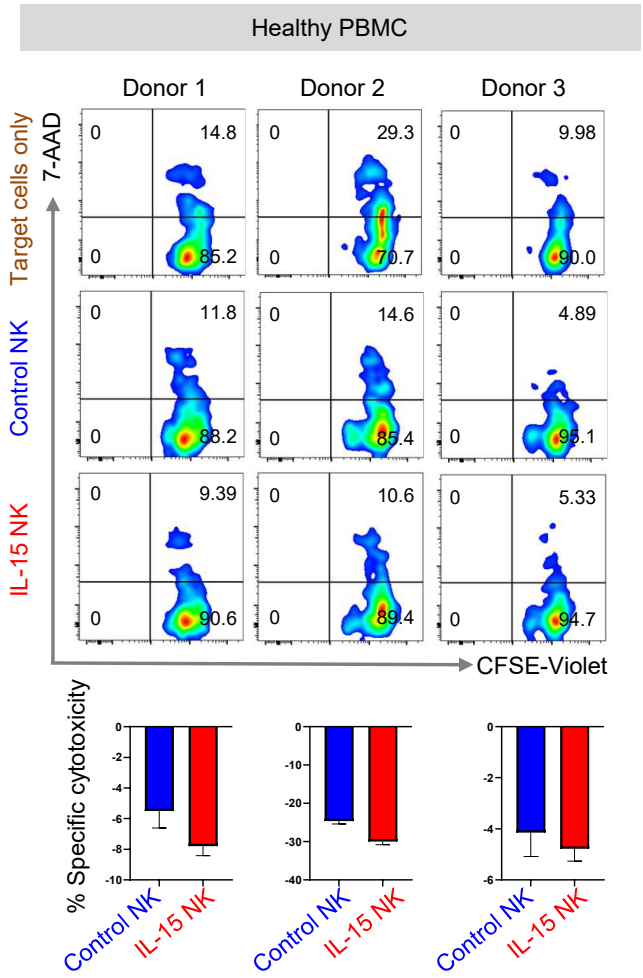

Figure S14: CRISPRa-engineered IL-15 NK cells are not toxic to healthy donor PBMC. Flow cytometry to compare specific cytotoxicity of dCas9-VP64-GFP$^+$ NK-92 cells transduced with control sgRNA-RFP (Control NK) or IL-15 sgRNA-RFP (IL-15 NK) against three independent healthy donor PBMC target cells. Effector: Target = 10:1. Comparisons were conducted using Student's t-test. Exact p-values are provided whenever significant (<0.05) or trending to significance (0.05<p<0.1).

Figure S15: *Inactivation of MYC restores autocrine IFN-I production and signaling in malignant human B cells*

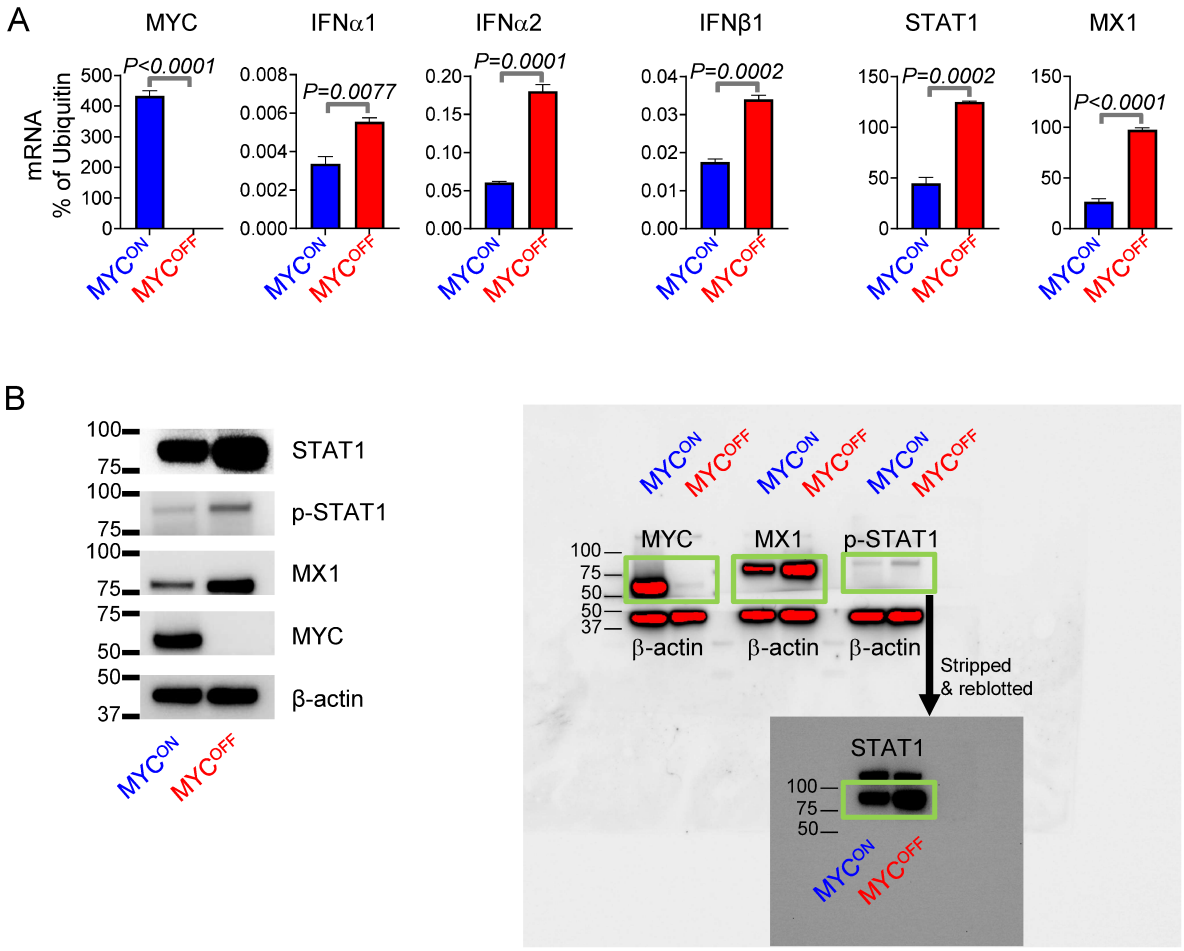

Figure S15: Inactivation of MYC restores autocrine IFN-I production and signaling in malignant human B cells. (**A**) Quantitation of expression of transcripts of MYC, IFNα1, IFNα2, IFNβ1, STAT1, and MX1 in MYC-overexpressing (MYC^{ON}) and MYC-inactivated (MYC^{OFF}) P493-6 malignant human B-cell line. Each qPCR sample was run in three technical replicates. The average of technical replicates is shown. P-values are calculated by unpaired t-test. Exact p-values are provided whenever significant (<0.05) or trending to significance (0.05<p<0.1). (**B**) Immunoblotting showing increase in global STAT1, p-STAT1, and MX1 after MYC inactivation in P493-6 cells (*left*). Full scan of blot (*right*).

Table S1: *List of B-ALL patient samples used in the study*

Patient ID	Age	Sex	Tissue Type	Cytogenetics	Translocation /Mutation status	Disease status	Source	Percentage of total IFNα2b^{+} cells
18067-HTB18-029	57	F	PBMC	Unknown	JAK2(G); JAK2(S) (Ph-like)	Diagnosis	City of Hope	0
18067-HTB19-1382	24	M	PBMC	Normal	EZH2; ETV6; KMT2D	Diagnosis	City of Hope	0
18067-LTB18-578	44	F	PBMC	Normal	KMT2D	Diagnosis	City of Hope	0.025
18067-HTB19-048	20	F	PBMC	47,XX,+22[6]	JAK2; JAK1 (Ph-like)	Diagnosis	City of Hope	0.055
18067-HTB19-937	41	F	PBMC	46,XX[16].ish t(X;14)(p22.33;q32.33)(5'IGH+;3'IGH+)[2]	IKZF1; JAK2(G); JAK2(S); PAX5 (Ph-like)	Diagnosis	City of Hope	0
18067-HTB19-376	30	F	PBMC	Unknown	KMT2D	Diagnosis	City of Hope	0.028
18067-HTB19-289	43	F	PBMC	47,XX,-2,t(3;15)(p23;q15),del(5)(q22q3?3),del(7)(p13p15),+del(9)(p21.2),der(9)del(9)(p13p22)del(9)(q22)x2,der(10)t(2;10)(q21;q26),del(12)(p11.2p13.3),add(17)(q25)x2,-20,+21,+mar[17]	KRAS; KMT2D; PAX5	Diagnosis	City of Hope	0.04
18067-LTB18-544	24	M	PBMC	47,XY,+X[6]	JAK2(G); JAK2(S) (Ph-like)	Diagnosis	City of Hope	0.014
18067-HTB19-1420	54	F	PBMC	46,XX,t(9;22)(q34.1;q11.2)[6];48,sl,+4,-16,+21,der(22)t(9;22) add (9)(q34.3),+der(22)t(9;22) add (9)[11] 47,sdl1,t(5;12)(q33;q13),-21[3]	KMT2C	Diagnosis	City of Hope	0.015

18067-HTB19-1424	25	Unknown	PBMC	46,XY,+X,der(1)dup(q42q12)?del(1)(q42q44),del(5)(q22q31),-7,t(8;9)(p21;q22),t(10;22)(p13;q13)[19]	KMT2D; NRAS; PAX 5	Diagnosis	City of Hope	0.012
65	33	F	Pheresis	47 - 48, xx, -4-11, +3-4 probable t(4;11)	*t(4;11) KMT2A* translocation	Diagnosis	University of Pennsylvania	
779	48	F	PBMC	46,XX,t(1;11)(p32;q23)[10]/48,idem,+X,+21[10]/FISH FOR MLL SPLIT POS 163/200 CELLS/FISH FOR BCR-ABL NEG 200 CELLS	*t(1;11) KMT2A* translocation	Diagnosis	University of Pennsylvania	
2142	30	M	Pheresis	46,XY,del(9)(p21p21)[6]/46,XY[24]	Ph-like	Diagnosis	University of Pennsylvania	
3113	44	F	PBMC	Unknown	*KMT2A/AFF1*	Diagnosis	University of Pennsylvania	
4986	41	M	PBMC	46,XY[5]	Ph-like	Diagnosis	University of Pennsylvania	
4988	61	F	PBMC	46,XX,del(7)(p11.2)[7]/46,XX[13]	Ph-like	Refractory	University of Pennsylvania	
18067-HTB19-1191	40	F	BMMC	50,XX,-2,add(3)(q27.3),+6,i(6)(p10),-10,+12,del(12)(q24.1),t(14;18)(q32.33;q21.33),+der(14)t(14;18),+17,+2mar[20].ish der(2)t(2;8)(q37;q24.21)(3'MYC+)[2]	KMT2D; PTMA-MYC	Diagnosis	City of Hope	0.012
18067-HTB19-525	66	M	BMMC	35,X,-Y,-3,-7,-8,-9,-13,-14,-15,-16,-17,-22[11]; Sideline 1: 35,sl,add(18)(p11.2),del(20)(q13.1q13.3)[4];	MLL2; TP53	Diagnosis	City of Hope	0.02
18067-HTB19-1130	24	Unknown	BMMC	47,X,-Y,t(4;11)(q21;q23.3),+6,del(7)(p11.2),+i(7)(q10),?add(21)(p11.2)[14]	KMT2A	Diagnosis	City of Hope	0
18067-HTB19-054	21	F	BMMC	47,XX,+22[6]	Jak2; Jak1	Diagnosis	City of Hope	0.069
18067-HTB1-004	48	M	BMMC	47,XY,+X,del(6)(q21q25),der(7)t(7;8)(p13;q22),i(17)(q10),5~11dmin.ish t(Y;14)(p11.3;q32.33)(5'IGH+;3'IGH	TP53	Diagnosis	City of Hope	0.058

				+)[3] Sideline: 47,sl,del(10)(q22q26)[3] Nonclonal aberrations of Sideline: add(X)(p22.1),add(X)(q24),add(5)(p11.2),del(8)(q11.2),add(7)(p11.2),+10,add(17)(p11.2				
18067-HTB22-0100	37	F	BMMC	46,XX,t(4;11;19)(q21;q23.3;q13.1)[13] Sideline 1: 46,sl,i(7)(q10)[4] Sideline 2: 47,sdl1,+21[3] Nonclonal Aberrations of Stemline and Sidelines: t(1;3)(p36.1;p21),t(1;6)(p36.1;q23),t(1;18)(p13;q11.2),add(2)(p13),add(3)(p13),add(6)(q21)	KMT2A, TP53, WHSC1	Diagnosis	City of Hope	0.012
18067-HTB22-0386	39	F	BMMC	38,XX,-2,-3,-4,del(5)(q22q33),-7,del(7)(q22q26),der(8)del(8)(p21)del(8)(q11.2q21.2),add(9)(p13),der(10)t(10;?12)(q26;q13),-12,-13,-15,-16,?der(17)t(12;17)(p1?1.2;q?21),der(21)t(3;21)(p21;q22.3)[cp5]	EP300, MUTYH, PAX5, TP53	Diagnosis	City of Hope	0.38

Table S2*: Reagents and antibodies used for flow cytometry*

Name	Fluorophore	Clone	Dilution/ Concentration	Source
Anti-human CD45	FITC	2D1	1:100	Biolegend
Anti-human CD3	BUV805	UCHT1	1:100	BD
Anti-human CD19	BUV661	HIB19	1:100	BD
Anti-human CD14	BUV395	M5E2	1:100	BD
Anti-human CD56	BV510	NCAM16.2	1:100	BD
Anti-human CD16	BV711	3G8	1:100	BD
Anti-human HLA-DR	BUV737	G-46-6	1:100	BD
Anti-human CD11c	BV605	3.9	1:100	BD
Anti-human CD123	PE/Cy7	6H6	1:100	BD
Anti-human IFN-α2b	APC	7N4-1	1:100	BD
Anti-human CXCR4	PECY5	12G5	1:100	Biolegend
Anti-pSTAT1 (pY701)	PE	4α	10:100	BD
Anti-mouse CD45	PerCP	30-F11	1:100	Biolegend
Anti-mouse CD19	APC	1D3	1:100	BD
Anti-mouse CD3	BUV395	17A2	1:100	BD
Anti-mouse CD8	BV711	53-6.7	1:100	Biolegend
Anti-mouse CD4	BV510	RM4-5	1:100	Biolegend
Anti-mouse Gr1	Alexa Fluor 700	RB6-8C5	1:100	Biolegend
Anti-mouse NKp46	PE	29A1.4	1:100	BD
Anti-mouse NK1.1	BV605	PK136	1:100	Biolegend
Anti-mouse PDCA1	BV750	927	1:100	BD
Anti-mouse CD11c	PC/CY7	N418	1:100	Biolegend
Anti-mouse CD27	BV650	LG.3A10	1:100	Biolegend
Anti-mouse CD11b	FITC	M1/70	1:100	Biolegend
Anti-mouse I-Ab	BUV805	25-9-17	1:100	BD
Ghost-Dye UV450	NA	NA	1:100	Tonbo Biosciences
CSFE-Violet	NA	NA	2.5μM	ThermoFisher Scientific
Perm Buffer IV 10X	NA	NA	0.5X	BD
BD Cytofix/Cytoperm fixation and permeabilization solution	NA	NA	1X	BD
7AAD	NA	NA	1:100	Biolegend
Fc block	NA	NA	1:100	BD
eBioscience™ Protein Transport Inhibitor Cocktail (500X)	NA	NA	1X	ThermoFisher SCIENTIFIC
ODN2395	NA	NA	3μM	InvivoGen

Table S3*: Reagents and antibodies used for mass cytometry*

Metal label	Target	Clone	Source	Concentration (µg/mL)	Titre (µg/mL)
141Pr	HLA-DR	L243	Custom, Biolegend	425	2
145Nd	CD4	RPA-T4	Fluidigm	500	5
146Nd	CD8	RPA-T8	Fluidigm	500	5
147Sm	CD20	2H7	Fluidigm	500	5
153Eu	CD45RA	HI100	Fluidigm	500	5
154Sm	CD3	UCHT1	Fluidigm	500	5
158Gd	CD33	WM53	Fluidigm	500	5
160Gd	CD14	M5E2	Fluidigm	500	5
166Er	IL-2	MQ1-17h12	Fluidigm	500	5
167Er	CD27	L128	Fluidigm	500	5
176Yb	CD56	NCAM16.2	Fluidigm	500	5
209Bi	CD16	3G8	Fluidigm	500	5

Table S4*: Primers used for qPCR analysis*

Name	Forward	Reverse
IFNαR1	CGAGGCGAAGTGGTTAAAAG	ACGGATCAACCTCATTCCAC
IFNαR2	ACCGTCTGCTTTTGATGGGT	AGAGGGTGTAGTTAGCGGGT
IFNβ1	GCCTTTGCCATCCAAGAGATGC	ACACTGTCTGCTGGTGGAGTT
IFNα1	GGATGTGACCTTCCTCAGACTC	ACCTTCTCCTGCGGGAATCCAA
IFNα2	ATCCAGAAGGCTCAAGCCATCC	GGAGGGTTGTATTCCAAGCAGC
STAT1	TGGTGAAATTGCAAGAGCTG	CAGACTTCCGTTGGTGGATT
MX1	CTCTGGGTGTGGAGCAGGAC	GAGGGCCACTCCAGACAGTG
IL-15	GTAGGTCTCCCTAAAACAGAGGC	TCCAGGAGAAAGCAGTTCATTGC
OAS1	GAGGTGGAGTTTGATGTGCTGC	GTGAAGCAGGTAGAGAACTCGC
Ubiquitin	AGCCCAGTGTTACCACCAAG	ACCCAAGAACAAGCACAAGG
IL-15 (Human)	AACAGAAGCCAACTGGGTGAATG	CTCCAAGAGAAAGCACTTCATTGC
MYC (Human)	CTGCGACGAGGAGGAGAACT	GGCAGCAGCTCGAATTTCTT
IFNα1 (Human)	TTGACTCATACACCAGGTCACG	AGCATGGTCATAGTTATAGCAGGG
IFNα2 (Human)	TGGGCTGTGATCTGCCTCAAAC	CAGCCTTTTGGAACTGGTTGCC
IFNβ1 (Human)	CTTGGATTCCTACAAAGAAGCAGC	TCCTCCTTCTGGAACTGCTGCA
STAT1 (Human)	CCGTTTTCATGACCTCCTGT	TGAATATTCCCCGACTGAGC
MX1 (Human)	GGCTGTTTACCAGACTCCGACA	CACAAAGCCTGGCAGCTCTCTA
Ubiquitin (Human)	GCCGCACTCTTTCTGACTACAAC	ACCTCCAGAGTGATGGTCTTGC

Table S5*: Antibodies used for immunoblotting*

Name	Clone ID/ Catalog No	Specificity	Dilution/ Concentration	Source
Anti-β-Actin	8H10D10	Mouse/Human	1:1000	Cell Signaling Technology
Anti-cMYC	D84C12	Mouse/Human	1:500	Cell Signaling Technology
Anti-phospho STAT1 (Ser727)	#9177S	Mouse/Human	1:500	Cell Signaling Technology
Anti-STAT1	#9172S	Mouse/Human	1:1000	Cell Signaling Technology
Anti-MX1	D3W71	Mouse/Human	1:1000	Cell Signaling Technology